Interoperability of phenome-wide multimorbidity patterns: a comparative study of two large-scale EHR systems

Nick Strayer[1*], Tess Vessels[2,3,4*], Karmel Choi[5,6], Siwei Zhang[1], Yajing Li[1], Brian Sharber[4], Ryan S Hsi[7], Cosmin A Bejan[8], Alexander G. Bick[4], Justin M Balko[4], Douglas B Johnson[4], Lee E Wheless[4], Quinn S Wells[4], Ravi Shah[4], Elizabeth J Philips[4,9], Wesley H Self [10,12], Jill M Pulley[11,12], Consuelo H Wilkins[4,12], Qingxia Chen[1], Tina Hartert[4], Michael R Savona[4], Yu Shyr[1], Dan M Roden[13], Jordan W Smoller[5,6,14], Douglas M Ruderfer[2,3,4,8,15], Yaomin Xu[1,8]

1. Department of Biostatistics, Vanderbilt University Medical Center, Nashville, TN, USA
2. Vanderbilt Genetics Institute, Vanderbilt University Medical Center, Nashville, TN, USA
3. Center for Digital Genomic Medicine, Vanderbilt University Medical Center, Nashville, TN, USA
4. Department of Medicine, Vanderbilt University Medical Center, Nashville, TN, USA
5. Psychiatric & Neurodevelopmental Genetics Unit, Center for Genomic Medicine, Massachusetts General Hospital, Boston MA
6. Center for Precision Psychiatry, Department of Psychiatry, Massachusetts General Hospital, Boston MA
7. Department of Urology, Vanderbilt University Medical Center, Nashville, TN, USA
8. Department of Biomedical informatics, Vanderbilt University Medical Center, Nashville, TN, USA
9. Institute for Immunology and Infectious Diseases, Murdoch University, Murdoch, Western Australia, Australia
10. Department of Emergency Medicine, Vanderbilt University Medical Center, Nashville, TN, USA
11. Department of Allergy, Pulmonary and Critical Care Medicine, Vanderbilt University School of Medicine, Nashville, TN, USA
12. Vanderbilt Institute for Clinical and Translational Research, Vanderbilt University Medical Center, Nashville, TN, USA
13. Department of Pharmacology, Vanderbilt University Medical Center, Nashville, TN, USA
14. Stanley Center for Psychiatric Research, Broad Institute, Cambridge, MA
15. Department of Psychiatry and Behavioral Sciences, Vanderbilt University Medical Center, Nashville, TN, USA

* Contribute equally

Correspondence to:
Yaomin Xu, Ph.D.
2525 West End Avenue, Suite 1100
Nashville, TN 37232
yaomin.xu@vumc.org
(615) 936-8199

Douglas M Ruderfer, Ph.D.
2525 West End Avenue, Suite 700
Nashville, TN 37232
douglas.ruderfer@vumc.org
(615) 875-9802

Keywords: multimorbidity, network analysis, electrical health records (EHR), real-world data analysis, cross-institutional interoperability, and reproducibility
Word Count: Abstract: 299, Body: 3119, References: 30

Abstract

Background: Electronic health records (EHR) are increasingly used for studying multimorbidities. However, concerns about accuracy, completeness, and EHRs being primarily designed for billing and administration raise questions about the consistency and reproducibility of EHR-based multimorbidity research.

Methods: Utilizing phecodes to represent the disease phenome, we analyzed pairwise comorbidity strengths using a dual logistic regression approach and constructed multimorbidity as an undirected weighted graph. We assessed the consistency of the multimorbidity networks within and between two major EHR systems at local (nodes and edges), meso (neighboring patterns), and global (network statistics) scales. We present case studies to identify disease clusters and uncover clinically interpretable disease relationships. We provide an interactive web tool and a knowledge base combing data from multiple sources for online multimorbidity analysis.

Findings: Analyzing data from 500,000 patients across Vanderbilt University Medical Center and Mass General Brigham health systems, we observed a strong correlation in disease frequencies (Kendall's $\tau = 0.643$) and comorbidity strengths (Pearson $\rho = 0.79$). Consistent network statistics across EHRs suggest a similar structure of multimorbidity networks at various scales. Comorbidity strengths and similarities of multimorbidity connection patterns align with the disease genetic correlations. Graph-theoretic analyses revealed a consistent core-periphery structure, implying efficient network clustering through threshold graph construction. Using hydronephrosis as a case study, we demonstrated the network's ability to uncover clinically relevant disease relationships and provide novel insights.

Interpretation: Our findings demonstrate the robustness of large-scale EHR data for studying complex disease interactions. The alignment of multimorbidity patterns with genetic data suggests the potential utility for uncovering shared etiology of diseases. The consistent core-periphery network structure offers a strategic approach to analyze disease clusters. This work also sets the stage for advanced disease modeling, with implications for precision medicine.

Funding: VUMC Biostatistics Development Award, UL1 TR002243, R21DK127075, R01HL140074, P50GM115305, R01CA227481

Introduction

Multimorbidity, the presence of multiple diseases within an individual, poses significant challenges for healthcare delivery and research[1,2]. Analysis of electronic health records (EHRs) offers a powerful approach to investigate complex multimorbidity patterns [3–5]. Understanding these patterns is crucial for revealing shared disease mechanisms, improving disease risk prediction, and optimizing clinical management[6–9]. However, concerns remain about the reproducibility of findings across diverse EHR systems, potentially hindering the translation of these insights into clinical practice.

Network analysis has emerged as a valuable tool for studying multimorbidity [10]. By modeling diseases as nodes and their co-occurrences as connections, these networks offer insights into disease relationships, clusters, and potential progression patterns. Yet, rigorous investigation of the consistency and theoretical foundation of these network models is needed to optimize their use in biomedical research. This study aims to address this gap through a comparative analysis of multimorbidity networks derived from two large-scale EHR systems. We assessed the reproducibility of disease comorbidity strengths and network structures,

explored the graph-theoretical implications of this analysis, and evaluated the performance of these networks in identifying disease clusters and elucidating disease relationships.

Our findings demonstrate the remarkable robustness of multimorbidity network analysis across EHRs. We observed strong conservation of network properties at multiple scales, including disease frequencies and comorbidity patterns (local), core-periphery structure (meso), and overall network statistics (global) (Figure 1A). These networks effectively identified clinically relevant disease clusters, and a case study on hydronephrosis revealed both known and potentially novel disease associations. Finally, we provide an interactive web-based tool to facilitate the exploration of these multimorbidity patterns and their cross-system comparisons.

Methods

EHR and disease phenome

Individual-level diagnostic code data for 250,000 randomly selected patients were gathered from Vanderbilt University Medical Center (VUMC) and Mass General Brigham (MGB)'s EHR systems of 2.2 million and 1.8 million patients at the time of data extraction, respectively. The sampled patients' longitudinal records were then collapsed to the number of occurrences of ICD9 and ICD10 codes. These code counts were mapped to phecodes v1.2 using the PheWAS R package [11]. Demographic data, including patient age at extraction date, EHR age (patient age at last recorded visit), sex, race, and the logarithm of the EHR burden (number of unique phecodes), were extracted for model adjustment. Those covariates help account for age-related disease patterns, healthcare utilization differences (indicated by EHR age and burden), and potential biases related to demographic differences reflected in sex and race. These covariate adjustments address the fact that the observed multimorbidity patterns are driven by

demographic factors or variations in healthcare utilization[1,12–14]. The study was approved by the Vanderbilt University Medical Center (VUMC) Institutional Review Board (IRB# 172041) and by the Mass General Brigham (MGB) Institutional Review Board (IRB# 2009P002312).

Dual regression analysis of disease comorbidities

We applied a dual logistic regression analysis strategy to characterize pairwise comorbidity strengths for each phecode pairs. Previous studies demonstrated the utility of regression model for large-scale comorbidity analysis[15]. This approach allows us to adjust for confounding factors that vary across institutions or populations, as well as differences in disease prevalence that could influence the accuracy of observed comorbidity frequencies. Our dual regression analysis include two regression models for each pair of phecodes (e.g., phecode A and B):

$$logit\big(P(B|A,Z)\big) = \beta_0 + \beta_1 A + \gamma Z \qquad (1)$$

$$logit\big(P(A|B,Z)\big) = \beta_0 + \beta_1 B + \gamma Z \qquad (2)$$

where Z represents covariates including patient age at the event, hospital usage in years, sex, race and the logarithm of disease burden. We extracted and averaged the test statistics (z-values) of the β_1 coefficients from the two regressions to generate a symmetric score for each phecode pair. This approach simplifies the complex nature of multimorbidity, enabling a structured evaluation of both disease association strengths and statistical significances while adjusting for potential confounders. This ensures robust findings, distinguishing true associations from spurious correlations within large EHR datasets and promoting generalizability across diverse populations.

Network model of phenome-wide multimorbidities

We model phenome-wide disease multimorbidities as undirected, weighted networks where diseases are nodes, and edges represent the pairwise comorbidity strengths derived from our dual regression analysis. Separate networks were constructed for VUMC and MGB EHR systems to enable comparative analysis and assess the consistency of multimorbidity patterns. This network modeling approach provides an intuitive foundation for understanding intricate multi-disease interactions, facilitates analyses such as disease cluster identification, disease progression modeling, and quantify disease importance within the multimorbidity network using graph-theoretic principles. This approach is computationally efficient, easier to visualize, and serves as a strategic starting point for characterizing complex disease-disease relationships. It offers a balance between simplicity and the ability to derive essential insights about complex disease relationships.

Structure equivalence in multimorbidity networks

We define a phecode's "multimorbidity pattern" as its set of comorbidity strengths to all other phecodes (Figure 1B). To quantify similarity between phecodes, considering both the magnitude of comorbidity strength and pattern of connections with neighboring nodes, we use a correlation-based structural equivalence measure[16]. Two phecodes are structurally equivalent if their multimorbidity patterns exhibit a high correlation, indicating similar relationships with other diseases within the network (Figure 1C). This approach characterizes nuanced meso-scale structures and positional roles of nodes within their neighboring nodes. It is often hypothesized that structurally equivalent nodes in a network will be similar in other ways such as sharing common mechanisms or functions.

Since our multimorbidity networks are constructed using identical phecode mappings, we can directly compare the structure equivalence measurements across two EHR systems. We calculate the "conservation " for each phecode as the correlation between its comorbidity strength vectors in the VUMC and MGB networks (Figure 1D). High conservation scores indicate consistent multimorbidity patterns across EHR systems, suggesting that the underlying mechanisms driving disease-disease relationships are transferable across the systems.

This intra- and inter- system structural equivalence analysis offers a novel approach to investigate multimorbidity relationships. By focusing on connection patterns with others, we move beyond simple pairwise comorbidities to uncover complex disease interactions and assess the generalizability of findings across diverse healthcare datasets.

Spectral analysis of multimorbidity network topology

We use network centrality measures to assess the global-scale topological consistency of multimorbidity networks across institutions. Eigenvector centrality, calculated from the leading eigenvector of the network adjacency matrix, quantifies a node's importance based on the number, strength, and importance of its connections in the network. Analyzing and comparing the distribution of centrality measures across the networks reveals the overall structure and their consistency[17]. Specifically, we consider the multimorbidity network as an undirected network of phecode nodes (phecode v1.2). The eigenvector centrality x_i of disease i is the ith element of the leading eigenvetor $\boldsymbol{x}$ of the network adjacency matrix $\mathbf{A}$, such that,

$$\mathrm{A}\boldsymbol{x} = \lambda_1 \boldsymbol{x}; \text{ where } \lambda_1 \text{ is the largest eigenvalue of } \mathbf{A} \qquad (3)$$

To evaluate meso-scale structure of the multimorbidity networks, we used eigengap heuristic[18]. This metric, defined as $1 - \lambda_2/\lambda_1$, where λ_1 and λ_2 are the largest and second largest eigenvalues of the network adjacency matrix $\mathbf{A}$, respectively, assesses how closely a network

resembles an ideal core-periphery model[19] (like a threshold graph). Higher eigengap values indicate a densely connected core, suggesting a prominent core-periphery structure.

Construction of consensus multimorbidity network

To facilitate cross-institutional analysis, we constructed a consensus multimorbidity network. Pairwise comorbidity strengths in this consensus network were calculated as weighted averages of the corresponding comorbidity strengths from the VUMC and MGB networks. Weights were proportional to the number of shared patients exhibiting each comorbidity pair in the respective system. For phecodes A and B, the combined pairwise comorbidity strength score is calculated as follows:

$$\text{combined comorbidity}_{A,B} = \frac{\left(\text{comorbidity}_{A,B}^{V} \cdot \mathrm{N}_{A,B}^{V}\right) + \left(\text{comorbidity}_{A,B}^{M} \cdot \mathrm{N}_{A,B}^{M}\right)}{\mathrm{N}_{A,B}^{V} + \mathrm{N}_{A,B}^{M}} \qquad (4)$$

where $\mathrm{N}_{A,B}^{V}$ and $\mathrm{N}_{A,B}^{M}$ are number of shared patients between phecodes A and B in VUMC and MGB cohorts, respectively. This weighting scheme prioritizes comorbidity estimates supported by larger patient populations, increasing the reliability of the consensus network.

Interactive online exploration of phenome-wide multimorbidities

We developed an interactive web application (https://prod.tbilab.org/PheMIME/) to facilitate the exploration of multimorbidity patterns across multiple EHR systems [20]. This tool allows users to visualize pairwise comorbidity patterns across institutions, examine the consistency of multimorbidity relationships across diverse EHR systems, and explore subgraph structures using associationSubgraphs [21]. This application provides researchers an intuitive interface to explore complex multimorbidity data, facilitating insights into disease relationships and the reproducibility of findings across different healthcare datasets.

Results

High concordance of disease frequencies and comorbidity strengths across EHR systems

We extracted demographic and clinical data (phecodes) for 250,000 randomly selected patients from de-identified EHRs at two healthcare systems (see Methods). The patient populations differed slightly in demographics, with VUMC having a higher proportion of females (55%) and white race (81%) compared to MGB (58% and 73%, respectively). Additionally, VUMC exhibited a younger median age (42.7 years) compared to MGB (52.6 years) likely due to a larger pediatric population (Table 1). Despite these demographic variations, disease frequencies exhibited a strong positive correlation across the phenome (Kendall's $\tau=0.643$, $p < 2.2e-16$). We observed higher diagnostic frequencies at VUMC, particularly within the "Sense Organs" category (Figure S1).

Table 1. Demographics of EHR patient cohorts

	VUMC: counts (percentage) (N=250,000)	MGB: counts (percentage) (N=250,000)
Age* Group(yrs)		
< 19	59,190 (23.68%)	7,613 (3.05%)
20 - 29	29,286 (11.71%)	24,878 (9.95%)
30 - 39	27,712 (11.08%)	37,563 (15.03%)
40 - 49	27,468 (10.99%)	41,166 (16.47%)
50 - 59	32,243 (12.90%)	44,962 (17.98%)
60 - 69	33,487 (13.39%)	41,922 (16.77%)
70 - 79	24,735 (9.89%)	29,577 (11.83%)
80 - 89	12,106 (4.84%)	18,289 (7.32%)
> 90	3,772 (1.51%)	4,030 (1.61%)
Age overall	**Mean (SD)**	**Mean (SD)**
	42.68 (24.37)	52.6 (19)
Race		
White	201,373 (80.55%)	185727 (74.29%)
Black	34,521 (13.81%)	16138 (6.46%)
Unknown	13,366 (5.35%)	17704 (7.08%)
Hispanic (not white)	514 (0.21%)	15967 (6.39%)
Other	140 (0.056%)	443 (0.18%)

	VUMC: counts (percentage) (N=250,000)	MGB: counts (percentage) (N=250,000)
Asian	69 (0.028%)	9435 (3.77%)
Native American/Alaskan	17 (0.0068%)	4586 (1.83%)
Sex		
Female	137,912 (55.17%)	144700 (57.88%)
Male	111,805 (44.72%)	105271 (42.11%)
Unknown	283 (0.11%)	29 (0.01%)
*Age when data exported from system, regardless of death status.		
†A Phecode is counted as "in record" when there are at least two observations of that Phecode over all the patient's records.		

We then calculated pairwise comorbidity strengths for all phecode pairs using the dual logistic regression approach (see Methods). The comorbidity strength scores demonstrated high concordance between the two EHRs (Pearson ρ=0.79; 95% CI: 0.787 – 0.794, Figure 2A). This indicates that the patterns of disease co-occurrence are remarkably consistent after adjusting for variations in patient populations and potential differences in healthcare practices.

Strong conservation of multimorbidity patterns across EHRs, with variations offering insights

We assessed the conservation of multimorbidity patterns across the two EHR systems using correlation-based structural equivalence (see Methods). High correlation scores indicate that a disease consistently co-occurs with the same set of diseases across EHRs. Specifically, we calculated Spearman correlations of phenome-wide multimorbidity patterns for each phecode with 500 bootstrap iterations to assess variability (Figure 2B). Overall, we observed strong conservation (median correlation = 0.772, Figure 2C). "Spinal stenosis" had the most conserved patterns (correlation = 0.942, CI = 0.921-0.958), while "Dental abrasion, erosion, and attrition" was the least conserved (correlation = -0.051, CI = -0.182-0.078). Examining conservation across categories, we found "Sense Organs" phecodes exhibited the lowest average conservation, while "Neoplasms" were the most conserved (Supplementary materials: A3). These variations in

conservation likely reflect differences in site-specific healthcare practices and patient populations.

High consistency of disease positions within multimorbidity networks

We assessed the consistency of diseases' topological positions within multimorbidity networks across EHRs using eigenvector centrality (see Methods). This metric quantifies a disease's importance based on the number, strength, and importance of its connections. We observed a high correlation in eigenvector centralities between VUMC and MGB (Spearman correlation = 0.902; 95% CI: 0.889 – 0.914, Figure 3A). This indicates a remarkable consistency in how diseases are positioned within the network structure. Examining the largest centrality differences, we found "Sense Organ" and "Respiratory" phecodes, such as "Cataract" and "Acute Sinusitis", tended to be more central in the VUMC network. In contrast, "Neoplasms" were significantly more central in the MGB network (Table S3, Figure S3). These patterns are further reflected in the distribution of eigen-centrality differences by category (Supplementary A5). Only "Neoplasms", "Musculoskeletal", and "Dermatologic" phecodes were, on average, more central in MGB.

Spectral analysis reveals core-periphery structure of multimorbidity networks

Spectral analysis revealed prominent core-periphery structures within the multimorbidity networks for both VUMC and MGB. This is evidenced by their large eigengaps (0.836 and 0.844) and consistently high eigenvector centralities across systems (see Methods, Figure 3B). In a core-periphery network, a densely connected core exists where diseases exhibit strong interconnections, while a sparsely connected periphery contains diseases with weaker links. Our UMAP representation (Figure 4) visually supports this interpretation, with musculoskeletal, metabolic, circulatory, and injuries & poisoning diseases enriched in the core.

This core-periphery structure implies a strategic analytical approach: isolating central disease clusters can identify more commonly occurring diseases in the population with shared mechanisms and functional overlaps, while investigating peripheral diseases could uncover more specific etiologies present only in subsets of patients. Furthermore, the networks' proximity to threshold graphs enables efficient search algorithms: applying the associationSubgraphs algorithm allowed us to dynamically cluster the multimorbidity networks, identifying subgraphs (disease clusters) even in cases where not all diseases within the cluster exhibit uniformly strong pairwise comorbidities, potentially uncovering broader and more clinically relevant disease clusters.

Multimorbidity patterns and genetic correlations of diseases strongly align

Genetically correlated diseases often share common pathophysiological mechanisms, potentially leading to elevated comorbidities. This suggests a link between multimorbidity patterns and shared disease etiology [22,23]. To investigate this connection, we analyzed the genetic correlation of 15 common, heritable phenotypes (Supplementary A9). Among the 105 phenotype pairs, 28 (26.7%) showed substantial genetic correlations (>0.5), including well-established pairs like "Coronary Atherosclerosis" and "Myocardial Infarction." We compared pairwise comorbidity strengths and multimorbidity similarity measures with their corresponding genetic correlations. Results revealed significant positive associations (Pearson correlations of 0.59 and 0.62, respectively; Figure 5). Notably, multimorbidity similarity demonstrated a stronger linear relationship with genetic correlation, suggesting it may be a more sensitive indicator of potential shared disease etiology, especially when direct comorbidity is weak.

Multimorbidity subgraphs identify robust disease clusters

We applied the associationSubgraphs method [21] to our multimorbidity networks to isolate disease clusters, or "subgraphs", representing groups of diseases with high co-occurrence rates (Supplementary A2). The consistent structural equivalence observed across different multimorbidity networks provides a strong theoretical basis for identifying clusters that are likely to be robust across different EHR systems and populations (Figure 4, Supplementary Figure S5). We identified several prominent disease condition clusters (Figure 6, Supplementary Tables S4-S6) that align with and refine previously reported condition clusters[24]. Examples include the cardiometabolic cluster (encompassing cardiovascular, metabolic diseases, and others), the mental health cluster (including mood disorders, anxiety, bipolar disorder, schizophrenia, substance use disorders, and others), and the musculoskeletal cluster (featuring conditions like back pain, fractures, sprains, and various joint disorders, and others). Additionally, we identified several large clusters (15+ phecodes) related to cancer, dermatological, reproductive, neurological, and eye disorders. Prior research links some of these clusters, like the mental health cluster, with poorer outcomes and increased healthcare costs [25].

Multimorbidity networks uncover disease relationships: A Hydronephrosis case study

We used hydronephrosis as a case study to demonstrate the utility of multimorbidity networks in revealing known and potentially novel disease relationships. Hydronephrosis is a kidney condition resulting from urinary tract obstruction [26]. We observed a strong conservation of multimorbidity patterns (conservation value: 0.852; 95% CI: 0.792 - 0.895, Figure 7A) and identified the strongest and most consistent comorbidities associated with hydronephrosis, including established causes like obstructing stones in the ureter, ureteral stricture, vesicoureteral reflux, congenital defects, and trauma [27] (Figure 7B, Supplementary Tables S7 & S8).

Additionally, we identified uncommon causes of hydronephrosis, such as cancers, pregnancy, urethral stricture, and abnormal renal vasculature [28–30]. Interestingly, the analysis also highlighted conditions with no known direct link to hydronephrosis, including pyelonephritis, E. coli, and Staphylococcus saprophyticus infections (Tables S7 & S8). These findings suggest the network's potential to identify novel disease associations for further investigation. These results can be explored interactively using our online application (https://prod.tbilab.org/PheMIME/).

Discussion

Our study demonstrates the robustness of EHR-derived multimorbidity analysis for investigating complex disease interrelations. We observed remarkable consistency in disease frequencies, comorbidity strengths, and multimorbidity network topologies across two large-scale, geographically distinct EHR systems. Such findings highlight the potential of EHR-based phenome-wide analysis to uncover complex disease-disease interactions, identify clinically relevant clusters, and their underlying shared disease mechanisms, despite the inherent variability in patient populations and healthcare practices.

The strong concordance of multimorbidity patterns after statistical adjustment for potential confounders provides compelling evidence for the reliability of this approach. Furthermore, the consistent core-periphery structure observed in both networks offers a strategic framework for analysis, suggesting disease clusters within the core may share common etiologies or risk factors, whereas diseases in the periphery may indicate more specific disease mechanisms unique to subsets of population.

The alignment of multimorbidity patterns with genetic correlations is particularly enlightening, supporting the notion that diseases with genetic linkages often share

pathophysiological pathways and exhibit higher comorbidity. This insight emphasizes the potential of multimorbidity networks to unravel intricate shared disease etiologies.

Despite the overall conservation of multimorbidity patterns, our analysis also unveiled notable differences, likely reflecting demographic and regional variations among patient populations. This underscores the importance of contextualizing multimorbidity analysis and interpretation within the specific framework of each EHR system, considering demographic factors, age distribution, and regional health trends.

The application of phecodes as disease phenome warrants specific consideration. Phecodes provide a standardized representation of diseases by grouping related ICD codes into broader, clinically relevant categories. Our results demonstrate that phecode-based multimorbidity analysis effectively captures reproducible disease relationships, supporting the use of phecodes in large-scale EHR studies for consistent and transferable insights into disease-disease relationships.

This study lays a methodological groundwork for future multimorbidity research. Our findings support the utility of multimorbidity networks for identifying disease clusters and exploring disease relationships. The case study on hydronephrosis demonstrated the network's ability to uncover both established and potentially novel disease associations, offering a potential tool for hypothesis generation.

Several limitations and areas for future research should be acknowledged. While informative, pairwise comorbidity analysis provides only an initial step into multimorbidity complexities. Future studies should investigate temporal disease progression patterns and incorporate additional data sources (e.g., laboratory results, medications) to refine our understanding of disease trajectories and causal relationships. Furthermore, while exploring the

influence of phecode organizational structure is beyond this study's scope, our null model simulations suggest minimal impact on network conservation (Supplementary A10). More in-depth analysis of how phenotype grouping methods affect findings warrants future investigation.

Overall, our comprehensive study offers compelling evidence for the reproducibility and applicability of EHR-based multimorbidity network analysis, laying the groundwork for precision medicine initiatives aimed at tailoring prevention and treatment strategies to the specific multimorbidity profile of individuals. The interactive web-based tool we introduce serves as a resource for the research community to further explore multimorbidity relationships, encouraging collaborations and accelerating discoveries in the field.

References

1. Pearson-Stuttard J, Ezzati M, Gregg EW. Multimorbidity—a defining challenge for health systems. *Lancet Public Health*. 2019;4(12):e599-e600. doi:10.1016/S2468-2667(19)30222-1
2. Skou ST, Mair FS, Fortin M, et al. Multimorbidity. *Nat Rev Dis Primers*. 2022;8(1):48. doi:10.1038/s41572-022-00376-4
3. Dong G, Feng J, Sun F, Chen J, Zhao XM. A global overview of genetically interpretable multimorbidities among common diseases in the UK Biobank. *Genome Med*. 2021;13(1):110. doi:10.1186/s13073-021-00927-6
4. Calvin CM, Conroy MC, Moore SF, Kuźma E, Littlejohns TJ. Association of Multimorbidity, Disease Clusters, and Modification by Genetic Factors With Risk of Dementia. *JAMA Netw Open*. 2022;5(9):e2232124. doi:10.1001/jamanetworkopen.2022.32124
5. Hassaine A, Canoy D, Solares JRA, et al. Learning multimorbidity patterns from electronic health records using Non-negative Matrix Factorisation. *J Biomed Inform*. 2020;112:103606. doi:10.1016/j.jbi.2020.103606
6. Brilleman SL, Salisbury C. Comparing measures of multimorbidity to predict outcomes in primary care: a cross sectional study. *Fam Pract*. 2013;30(2):172-178. doi:10.1093/fampra/cms060
7. Salisbury C, Johnson L, Purdy S, Valderas JM, Montgomery AA. Epidemiology and impact of multimorbidity in primary care: a retrospective cohort study. *British Journal of General Practice*. 2011;61(582):e12-e21. doi:10.3399/bjgp11X548929
8. Lehnert T, Heider D, Leicht H, et al. Review: Health Care Utilization and Costs of Elderly Persons With Multiple Chronic Conditions. *Medical Care Research and Review*. 2011;68(4):387-420. doi:10.1177/1077558711399580

9. Langenberg C, Hingorani AD, Whitty CJM. Biological and functional multimorbidity—from mechanisms to management. *Nat Med*. 2023;29(7):1649-1657. doi:10.1038/s41591-023-02420-6
10. Fotouhi B, Momeni N, Riolo MA, Buckeridge DL. Statistical methods for constructing disease comorbidity networks from longitudinal inpatient data. *Appl Netw Sci*. 2018;3(1):46. doi:10.1007/s41109-018-0101-4
11. Carroll RJ, Bastarache L, Denny JC. R PheWAS: data analysis and plotting tools for phenome-wide association studies in the R environment. *Bioinformatics*. 2014;30(16):2375-2376. doi:10.1093/bioinformatics/btu197
12. Marengoni A, Angleman S, Melis R, et al. Aging with multimorbidity: A systematic review of the literature. *Ageing Res Rev*. 2011;10(4):430-439. doi:10.1016/j.arr.2011.03.003
13. Rodrigues LP, Vissoci JRN, França DG, et al. Multimorbidity patterns and hospitalisation occurrence in adults and older adults aged 50 years or over. *Sci Rep*. 2022;12(1):11643. doi:10.1038/s41598-022-15723-4
14. Soley-Bori M, Ashworth M, Bisquera A, et al. Impact of multimorbidity on healthcare costs and utilisation: a systematic review of the UK literature. *British Journal of General Practice*. 2021;71(702):e39-e46. doi:10.3399/bjgp20X713897
15. Arias-de la Torre J, Ronaldson A, Prina M, et al. Depressive symptoms during early adulthood and the development of physical multimorbidity in the UK: an observational cohort study. *Lancet Healthy Longev*. 2021;2(12):e801-e810. doi:10.1016/S2666-7568(21)00259-2
16. Newman M. *Networks*. Vol 1. Oxford University Press; 2018. doi:10.1093/oso/9780198805090.001.0001
17. Cvetkovic D, Rowlinson P, Simic S. *Eigenspaces of Graphs*. Cambridge University Press; 1997. doi:10.1017/CBO9781139086547
18. von Luxburg U. A tutorial on spectral clustering. *Stat Comput*. 2007;17(4):395-416. doi:10.1007/s11222-007-9033-z
19. Schoch D, Valente TW, Brandes U. Correlations among centrality indices and a class of uniquely ranked graphs. *Soc Networks*. 2017;50:46-54. doi:10.1016/j.socnet.2017.03.010
20. Zhang S, Strayer N, Vessels T, et al. PheMIME: An Interactive Web App and Knowledge Base for Phenome-Wide, Multi-Institutional Multimorbidity Analysis. *medRxiv*. Published online January 1, 2023:2023.07.23.23293047. doi:10.1101/2023.07.23.23293047
21. Strayer N, Zhang S, Yao L, et al. Interactive network-based clustering and investigation of multimorbidity association matrices with associationSubgraphs. *Bioinformatics*. 2023;39(1). doi:10.1093/bioinformatics/btac780
22. Bulik-Sullivan B, Finucane HK, Anttila V, et al. An atlas of genetic correlations across human diseases and traits. *Nat Genet*. 2015;47(11):1236-1241. doi:10.1038/ng.3406
23. van Rheenen W, Peyrot WJ, Schork AJ, Lee SH, Wray NR. Genetic correlations of polygenic disease traits: from theory to practice. *Nat Rev Genet*. 2019;20(10):567-581. doi:10.1038/s41576-019-0137-z
24. Prados-Torres A, Calderón-Larrañaga A, Hancco-Saavedra J, Poblador-Plou B, van den Akker M. Multimorbidity patterns: a systematic review. *J Clin Epidemiol*. 2014;67(3):254-266. doi:10.1016/j.jclinepi.2013.09.021

25. Lehnert T, Heider D, Leicht H, et al. Review: Health Care Utilization and Costs of Elderly Persons With Multiple Chronic Conditions. *Medical Care Research and Review*. 2011;68(4):387-420. doi:10.1177/1077558711399580
26. Patel K, Batura D. An overview of hydronephrosis in adults. *Br J Hosp Med*. 2020;81(1):1-8. doi:10.12968/hmed.2019.0274
27. Kass EJ, Silver TM, Konnak JW, Thornbury JR, Wolfman MG. The Urographic Findings in Acute Pyelonephritis: Non-Obstructive Hydronephrosis. *Journal of Urology*. 1976;116(5):544-546. doi:10.1016/S0022-5347(17)58904-1
28. Stephens FD. Ureterovascular Hydronephrosis and the "Aberrant" Renal Vessels. *Journal of Urology*. 1982;128(5):984-987. doi:10.1016/S0022-5347(17)53308-X
29. Rasmussen PE, Nielsen FR. Hydronephrosis during pregnancy: a literature survey. *European Journal of Obstetrics & Gynecology and Reproductive Biology*. 1988;27(3):249-259. doi:10.1016/0028-2243(88)90130-X
30. Ilgi M, Bayar G, Abdullayev E, et al. Rare Causes of Hydronephrosis in Adults and Diagnosis Algorithm: Analysis of 100 Cases During 15 Years. *Cureus*. Published online May 21, 2020. doi:10.7759/cureus.8226

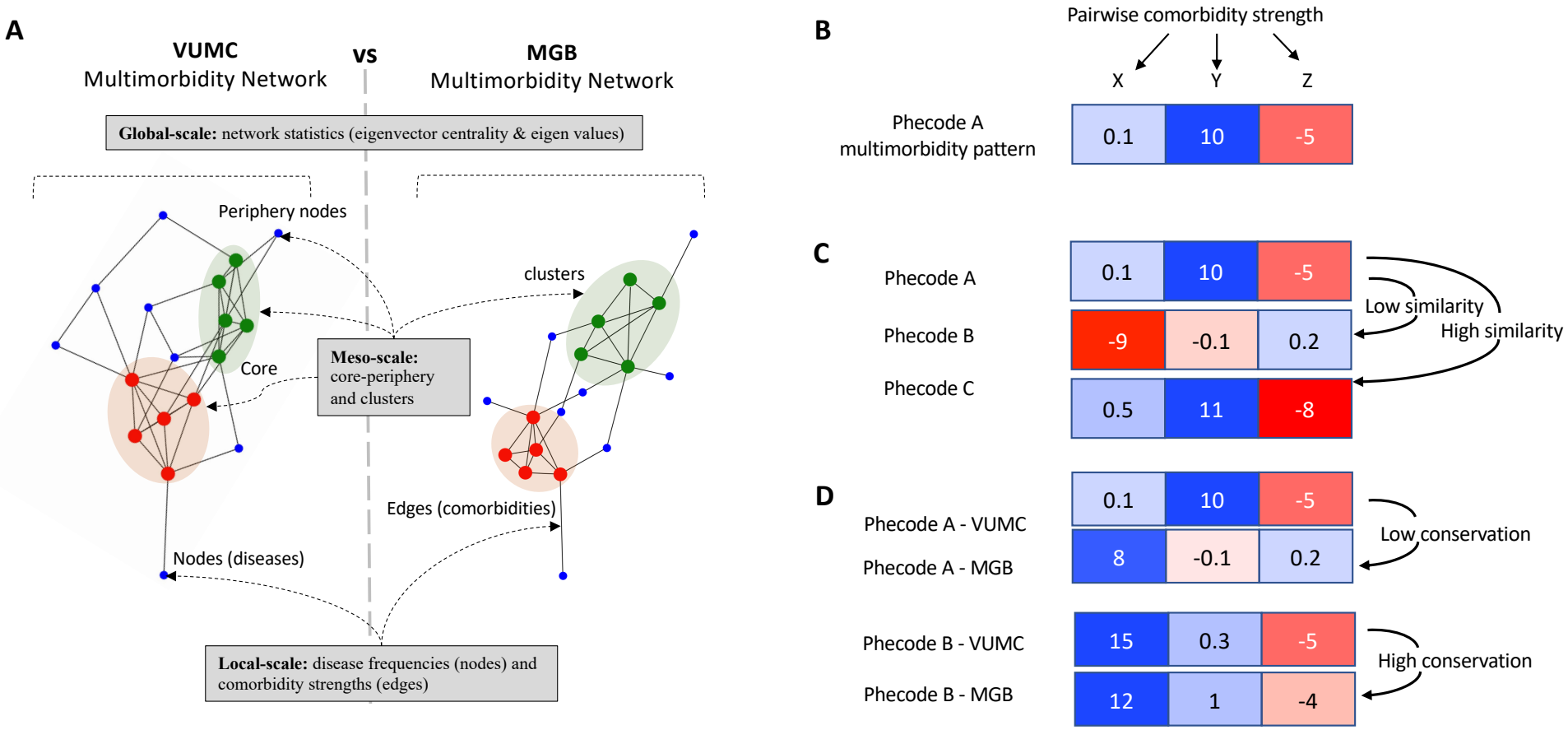

Figure 1. Schematic demonstration of multimorbidity networks, connection patterns, similarity, and conservation. A. Network Structure: Multimorbidity networks visualize diseases (nodes) and their pairwise comorbidity strengths (edge weights). Global scale investigation utilizes network statistics to characterize the overall shape and connectivity of the entire network, the meso-scale features describe intermediate structures like core-periphery patterns (where diseases cluster in a densely connected core or a less connected periphery) or other distinct disease clusters, and the local scale patterns focus on individual diseases and their immediate connections. **B. Multimorbidity Patterns:** A single disease (phecode A) exhibits a unique pattern of comorbidity strengths with other diseases (X, Y, Z). **C. Multimorbidity Similarity:** Similarity assesses how closely two diseases' comorbidity patterns align within the network. Here, phecode A is more similar to C than B. **D. Conservation Across EHR Systems:** Conservation examines how consistently multimorbidity patterns replicate across different datasets. Phecode B's pattern is highly conserved between EHR systems, while A's is less so.

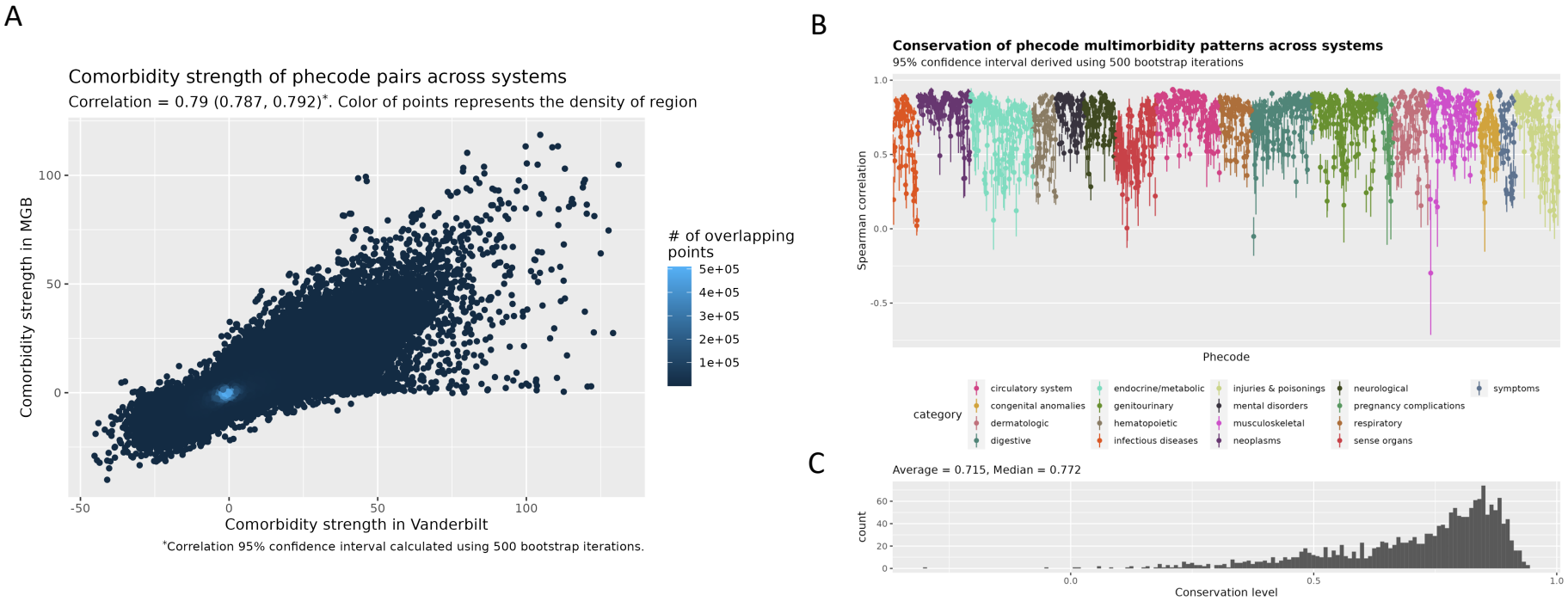

Figure 2. High conservation of multimorbidity patterns across EHR Systems. A. Consistency of Comorbidity Strengths: Scatterplot demonstrates strong correlation between pairwise comorbidity strengths for all common phecode pairs across Vanderbilt and MGB systems. This indicates that diseases with high (or low) comorbidity in one EHR tend to exhibit a similar pattern in the other. **B. Conservation of Structure Equivalence:** Measures how consistently a disease's connection with others within the multimorbidity network aligns across the EHR systems. The dots represent bootstrap means, with confidence intervals indicating uncertainty. Most phecodes exhibit high correlation, demonstrating a conserved role within the networks. **C. Distribution of Conservation:** The skewed distribution of bootstrap means towards 1 highlights a strong trend of structure equivalence conservation across EHR systems, supporting the reproducibility of multimorbidity networks.

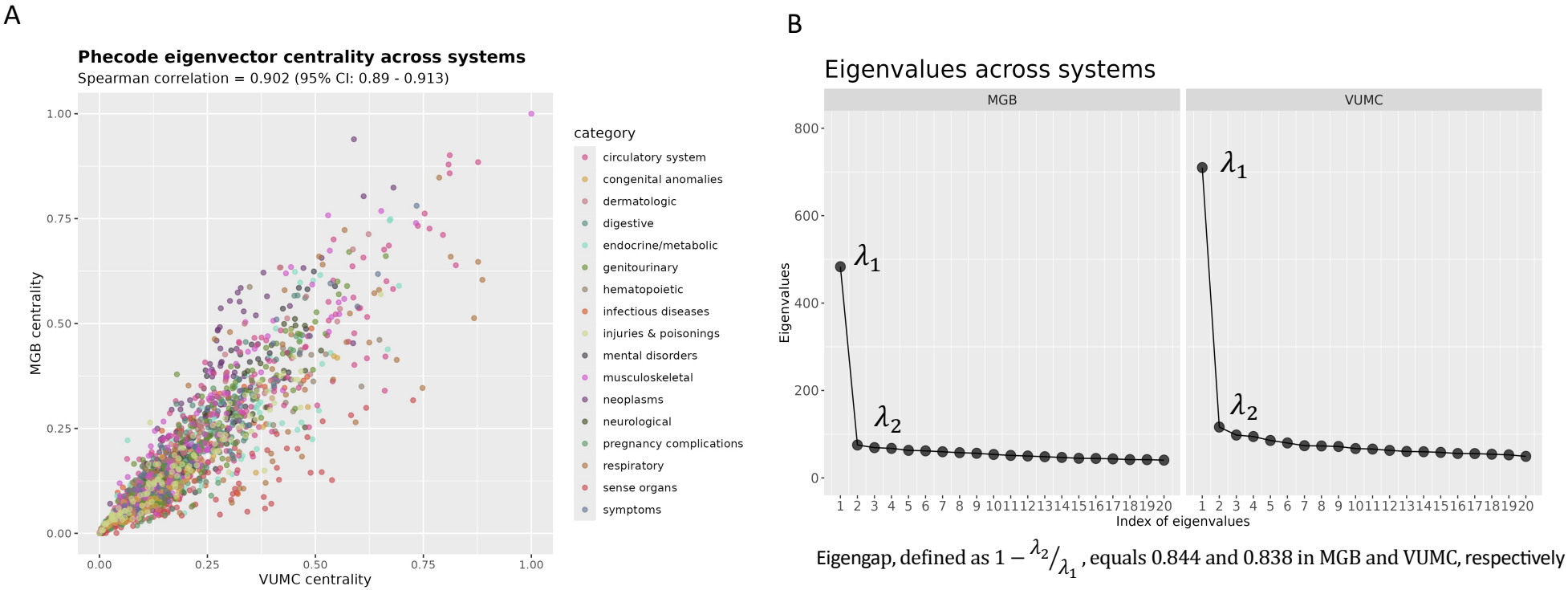

Figure 3. Consistent Spectral Properties of Multimorbidity Networks. A. Conserved Eigenvector Centrality: Eigenvector centrality scores, which reflect a disease's importance within the network, are strongly correlated across the two EHR systems. This indicates most diseases maintain similar roles in the multimorbidity networks. Notable differences exist in the "sense organs" category, likely reflecting dataset-specific factors. **B. Consistent Eigengaps:** Eigengaps, which help identify core-periphery structure, are consistent across both systems. This further supports the robust conservation of multimorbidity network patterns.

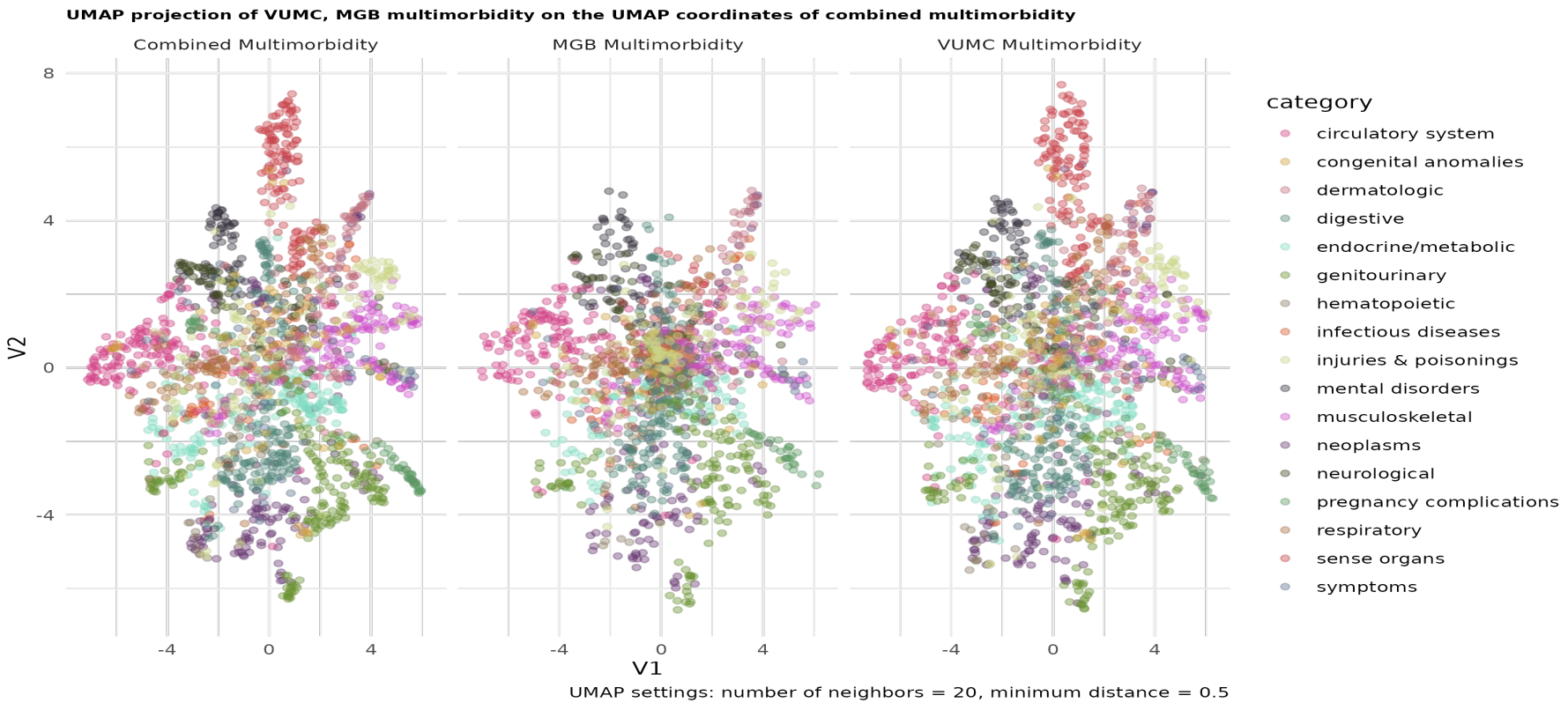

Figure 4. UMAP Visualization Reveals Consistent Multimorbidity Network Structure with Dataset-specific Variation. UMAP projection of multimorbidity networks reveals remarkable consistency in their overall structure across EHR systems. Both networks exhibit a prominent core-periphery structure. Phecodes cluster according to their disease categories (e.g., circulatory, musculoskeletal), and more nuanced clustering patterns are also consistently observed within these categories. Despite the overall consistency, dataset-specific differences exist, such as the "sense organs" cluster that is notably more prominent in the VUMC network.

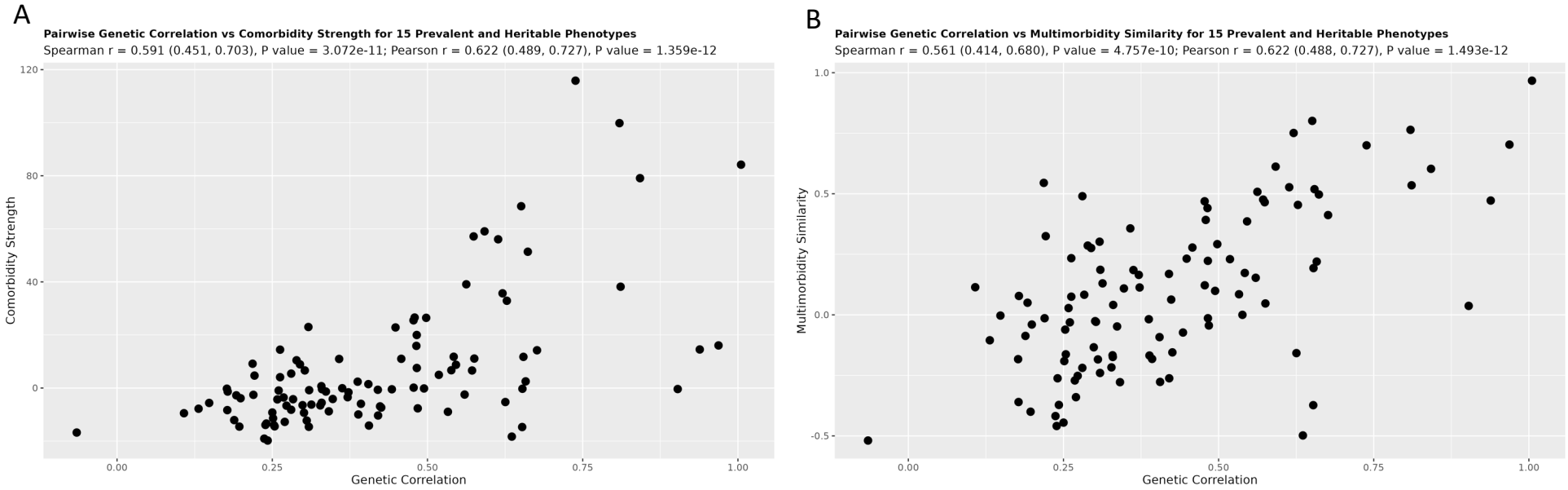

Figure 5. Comorbidity Strength and Multimorbidity Similarity Aligns with Genetic Correlation. Scatterplots comparing phenotypic similarity measures (based on multimorbidity patterns) with genetic correlations for 15 prevalent, heritable phenotypes. **A. Comorbidity Strength vs. Genetic Correlation:** Demonstrates a significant positive association between pairwise comorbidity strengths and genetic correlations. **Multimorbidity Similarity vs. Genetic Correlation:** Exhibits an even stronger positive association, suggesting that multimorbidity similarity may be a more sensitive indicator of shared disease etiology, especially where direct comorbidity is weak.

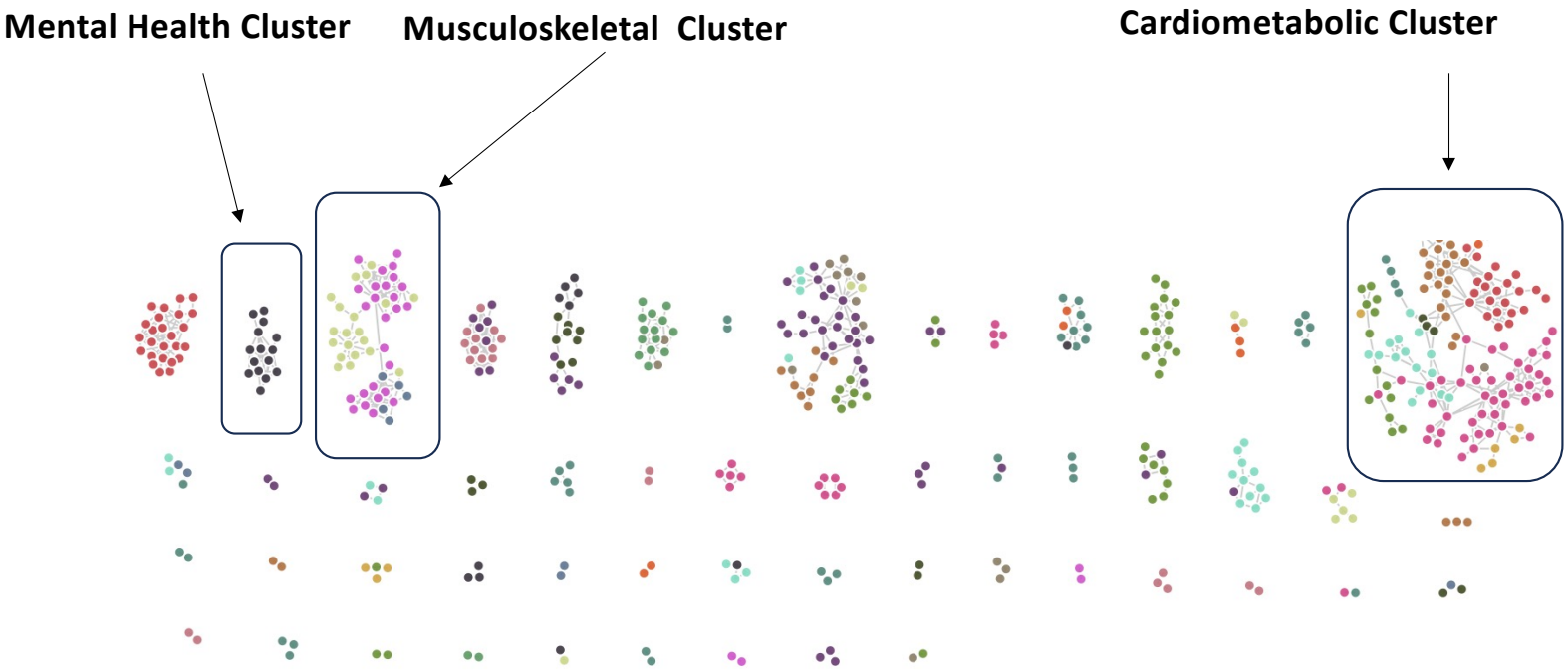

Figure 6. Multimorbidity Network Analysis Identifies Robust Disease Clusters. AssociationSubgraphs analysis of the consensus phenome-wide multimorbidity network reveals several prominent disease clusters (or "condition clusters") that align with those consistently found across multiple studies. Highlighted clusters include the Cardiometabolic Cluster (encompassing cardiovascular and metabolic diseases), the Mental Health Cluster (including mood disorders, depression, anxiety, and other mental health conditions), and the Musculoskeletal Cluster (featuring musculoskeletal disorders and injuries).

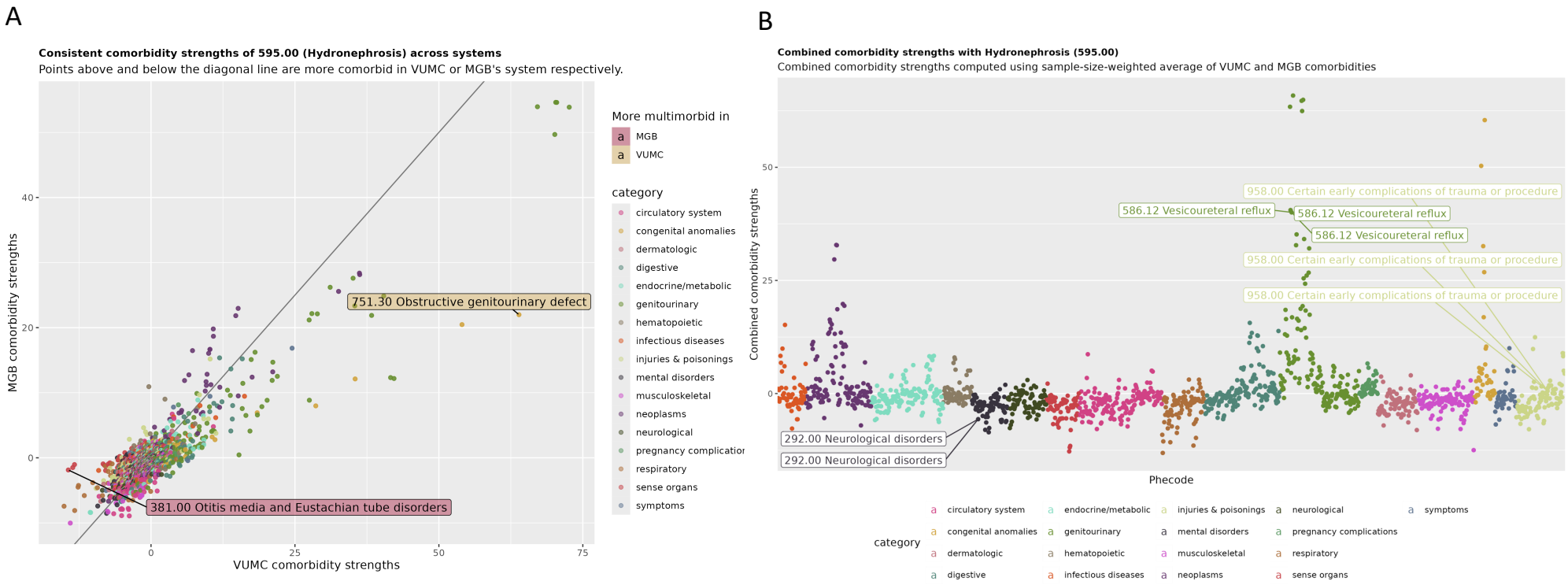

Figure 7. Multimorbidity Landscape of Hydronephrosis. A. Analysis reveals a largely consistent comorbidity landscape for hydronephrosis across both EHR systems. **A.** Pairwise comorbidity strengths are highly aligned, with minor variations in the extreme end of the distribution (e.g., obstructive genitourinary defects being slightly more comorbid in the Vanderbilt dataset). **B.** Consistent Phecode Comorbidity Strength identifies highly comorbid conditions, including expected associations such as obstructing stones, vesicoureteral reflux, neurological conditions, and trauma, along with rarer causes and potentially novel conditions.